Cs + reactive scattering from a Si(111) surface adsorbed with water

M. C. Yang, C. H. Hwang, and H. Kang

Citation: The Journal of Chemical Physics **107**, 2611 (1997); doi: 10.1063/1.474572
View online: http://dx.doi.org/10.1063/1.474572
View Table of Contents: http://scitation.aip.org/content/aip/journal/jcp/107/7?ver=pdfcov
Published by the AIP Publishing

Cs^+ reactive scattering from a Si(111) surface adsorbed with water

M. C. Yang, C. H. Hwang, and H. Kang[a)]
Department of Chemistry, Pohang University of Science and Technology, Pohang, Gyeongbuk 790-784, South Korea

(Received 4 April 1997; accepted 7 May 1997)

Reactive scattering of hyperthermal Cs ion is examined from a Si(111) surface adsorbed with water. Collision of Cs^+ beams with the Si surface at the energy of 10–100 eV produces Cs^+-bound cluster ions as scattering products, including $CsOH^+$, $CsOH_2^+$, $CsSi^+$, $CsSiH_n^+$ ($n=1,2$), and $CsSiO^+$. The yields for these clusters are examined as a function of Cs^+ beam energy and water exposure. Kinetic energy distributions for the clusters are measured. The reactive scattering process is explained in terms of collision-induced desorption of adsorbate, followed by ion–molecule association between the scattered Cs^+ and the desorbed molecule. The probability that Cs^+ undergoes reactive scattering is $5\times10^{-4}-2\times10^{-3}$ for 50 eV collision energy. The corresponding probability for the Cs^+–molecule association reaction is in the order of $5\times10^{-3}-2\times10^{-2}$ or slightly lower. It is proposed that $CsOH^+$ and $CsOH_2^+$ are formed from OH and H_2O adsorbates, respectively, via direct collisional desorption. $CsSiO^+$ formation can be related to desorption of surface oxide species or, at high energy, to collisional dissociation of adsorbates. Several aspects of using Cs^+ reactive scattering for surface adsorbate detection are discussed. © *1997 American Institute of Physics.* [S0021-9606(97)02131-4]

I. INTRODUCTION

During the past years many endeavors have been made in order to understand gas–surface collisional phenomena. The collisional nature varies depending on the particle energy from trapping and desorption in the thermal regime to binary collision (BC) in the keV energy range.[1] Between these two extremes, there exists a transitional region, often called hyperthermal energy (1–100 eV). Gas–surface interactions in this energy region offers an interesting subject to explore, not only because such investigation can bridge the gap between thermal and BC collisional behaviors, but because chemical transformation energy falls into this region. Recent investigations of hyperthermal gas–surface interactions to pursue such aims have been well responded. Hyperthermal collision, induces dissociation of molecular projectiles,[2–10] desorption from surface,[11–19] chemical reaction with functionalized surface,[3,4] and surface modification and film deposition in the atomic scale.[20–23]

Recently, we reported that Cs^+ ions of hyperthermal energy undergo reactive scattering from a solid surface,[24,25] producing Cs^+-bound clusters (CsX^+, where X is an adsorbate or a surface atom). We proposed that the reactive scattering process can conceptually be divided into two steps,[24,25]

$$Cs^+(g)+X\text{–surface}\rightarrow Cs^+(g)+X(g)+\text{surface} \quad \text{(reaction 1)}$$

$$Cs^+(g)+X(g)\rightarrow CsX^+(g). \quad \text{(reaction 2)}$$

In reaction 1, collision of hyperthermal Cs^+ causes desorption of X from the surface. Then, the desorbed X is attracted to the scattered Cs^+ via electrostatic attraction forces, and forms a CsX^+ complex (reaction 2). In this paper, we present detailed experimental results and analyses for Cs^+–surface reactive scattering. Various Cs^+-bound cluster ions emanating from a water-adsorbed Si(111) surface are identified, and their yields are measured as a function of beam collision energy and water exposure. The kinetic energies of the cluster ions are measured. These results are analyzed in order to understand the dynamics of reactive scattering.

The water-adsorbed Si surface is an important system to study because it is related to the initial stage of wet Si oxidation, a process useful in semiconductor industry. Despite numerous studies in the past years, subtle questions still remain regarding the adsorption state of water on Si. An excellent review on the interaction of water with Si surfaces has been done by Thiel and Madey.[26] We will only briefly mention several representative studies on this subject. Ultraviolet photoelectron spectroscopic (UPS) studies have suggested that H_2O adsorbs molecularly on a Si surface,[27,28] together with some hints for partial dissociation.[29] On the other hand, high resolution electron energy loss spectroscopy (HREELS) indicates mostly dissociated OH,[30,31] probably due to instrumental difficulty of detecting molecular H_2O.[32] Laser induced thermal desorption (LITD) (Refs. 33,34) has detected H_2O and SiOH moieties desorbing from a Si(111)-7×7 surface, supporting partial dissociation of H_2O. Scanning tunneling microscopic (STM) study[35] suggests molecular adsorption at low water coverages ($\theta<0.05$ ML) while dissociative adsorption at high coverages ($\theta>0.1$ ML). Recent X-ray photoelectron spectroscopic (XPS) study using synchrotron radiation[36] shows that H_2O not only dissociates into H and OH on the (111)-7×7 surface, but oxidation of Si to oxides can also occur at high water exposures. To summarize the results to the present, at least a certain fraction of water molecules are believed to exist in dissociated forms on a room temperature Si(111)-7×7 surface. For high water ex-

[a)]Author to whom correspondence should be addressed. FAX: +82-562-279-3399. Electronic mail: surfion@vision.postech.ac.kr

posure, a small amount of surface oxides may also be formed.

II. EXPERIMENT

The experiment was performed using the ion–surface scattering chamber equipped with a low-energy (1–300 eV) ion beamline. This apparatus has previously been described in detail.[7,37] Cs^+ ions were produced from CsCl powder heated inside the Colutron ion source. The ion beam was mass-selected by a Wien filter and electrostatically deflected to eliminate possible neutral impurities before it reached the sample surface. A Faraday cup was used to spatially probe the profile of the beam and to measure ion current density. The current density of the Cs^+ beam was $1-10\ \mathrm{nA\ cm^{-2}}$, and its energy spread was normally less than 2 eV. The sample, an intrinsic phosphorus-doped Si(111) wafer with its area of 1 cm×1 cm, was placed inside an electric field-free region of the scattering chamber. The native oxide layer was removed from the sample surface by cycles of Ar^+ sputtering at 2 keV and heating at 1100 °C using electron bombardment from the backside in ultrahigh vacuum (UHV). The sample prepared in this fashion has a (111)-7×7 reconstructed surface.[22] Once a clean surface was prepared in UHV, heating to 1100 °C was sufficient to remove the impurities adsorbed during the experiment. Surface cleanness was checked by Auger electron spectroscopy (AES) and Cs^+ reactive scattering. The cleaned surface was then exposed to water vapor at a pressure of 1×10^{-6} Torr at room temperature.

The ions scattered from the surface were detected using a quadrupole mass spectrometer (QMS) operated in a positive ion sampling mode. Kinetic energy of the ions was measured by placing a retarding field analyzer (RFA) of a 4-grid type in front of the mass spectrometer nose. The angle between an incident ion beam and a detector was fixed at 90°, and the incidence beam direction was 45° to the surface. The total Cs^+ beam dose was kept less than 1×10^{14} ions $\mathrm{cm^{-2}}$ in most experiments. The base pressure of the UHV scattering chamber was 3×10^{-10} Torr. Through differential pumping of the beamline, the chamber pressure was maintained in the 10^{-10} Torr range during Cs^+ beam exposure.

III. RESULTS

A. Mass identification of Cs^+-bound clusters

Collision of hyperthermal Cs^+ ions onto a water-adsorbed Si(111) surface gives rise to various CsX^+ cluster ions. Figure 1 shows the cluster species produced from the surface exposed to water vapor up to saturation (1000 L, $1\ \mathrm{L}=1\times10^{-6}$ Torr s) at room temperature. The mass spectra are displayed for the region of 130–200 amu. In the lower mass region, no peaks appear with measurable intensity except H^+ and alkali metal ions produced from surface impurities. The spectra of Fig. 1 are characterized by an intense Cs^+ peak at 133 amu and the higher mass peaks representing CsX^+ cluster ions. Upon 15 eV Cs^+ collision onto the H_2O-adsorbed surface, three cluster ions appear that are

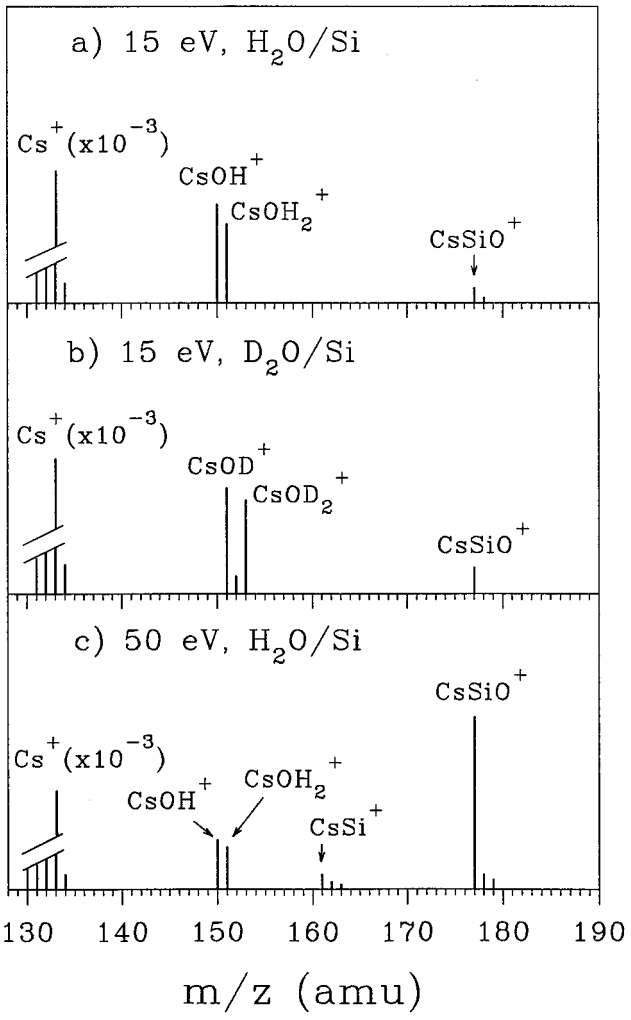

FIG. 1. Mass spectra of the positive ions emitted upon Cs^+ impact of a Si(111) surface adsorbed with water at saturation coverage. The intensity of the scattered Cs^+ peak is reduced to a factor 1×10^{-3}. The angles of an incident Cs^+ beam and a detector are 45° to the surface normal. (a) 15 eV collision on H_2O-adsorbed surface. (b) 15 eV collision on D_2O-adsorbed surface. (c) 50 eV collision on H_2O-adsorbed surface.

identified as $CsOH^+$ (150), $CsOH_2^+$ (151), and $CsSiO^+$ (177 amu) [Fig. 1(a)]. The intensities of these products are $10^{-3}-10^{-4}$ times smaller than the elastically scattered Cs^+. In order to confirm the mass identification, a control experiment has been performed by exposing a surface with D_2O. The $CsOH^+$ and $CsOH_2^+$ peaks become shifted to 151 and 153 amu, representing $CsOD^+$ and $CsOD_2^+$, respectively [Fig. 1(b)]. The $CsSiO^+$ peak remains in the same position (177 amu). A small peak at 152 amu is attributed to $CsOHD^+$ coming from adsorbed HDO impurity. It is because a small HDO partial pressure was measured during D_2O exposure, possibly produced from isotope scrambling reactions on stainless steel chamber walls. The isotopic substitution does not change the intensity ratio $I(CsOD^+)/I(CsOD_2^+)$ from $I(CsOH^+)/I(CsOH_2^+)$. CsD^+ ions (135 amu) are not emitted or have only negligible in-

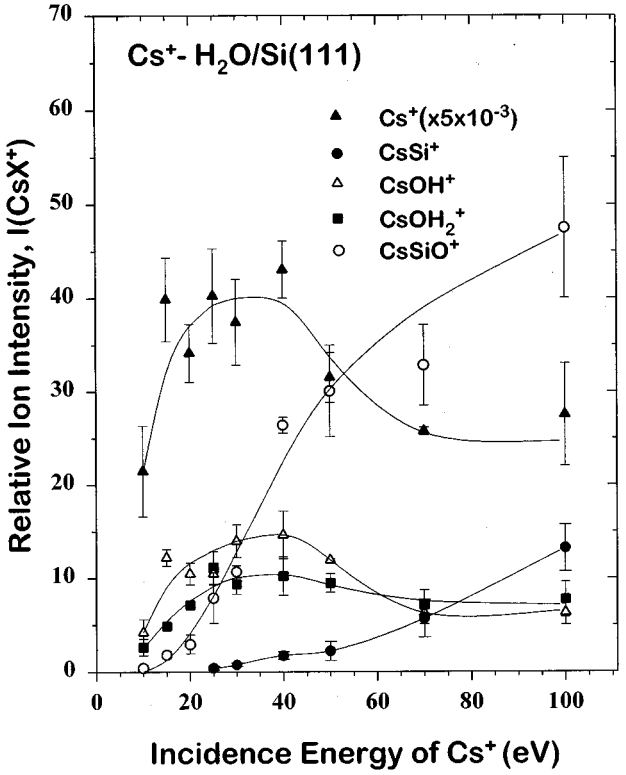

FIG. 2. Ion emission intensities for Cs^+ (▲), $CsOH^+$ (△), $CsOH_2^+$ (■), $CsSi^+$ (●), and $CsSiO^+$ (○) as a function of Cs^+ beam energy for the range of 10–100 eV. The intensities are normalized to the Cs^+ current reading at the sample.

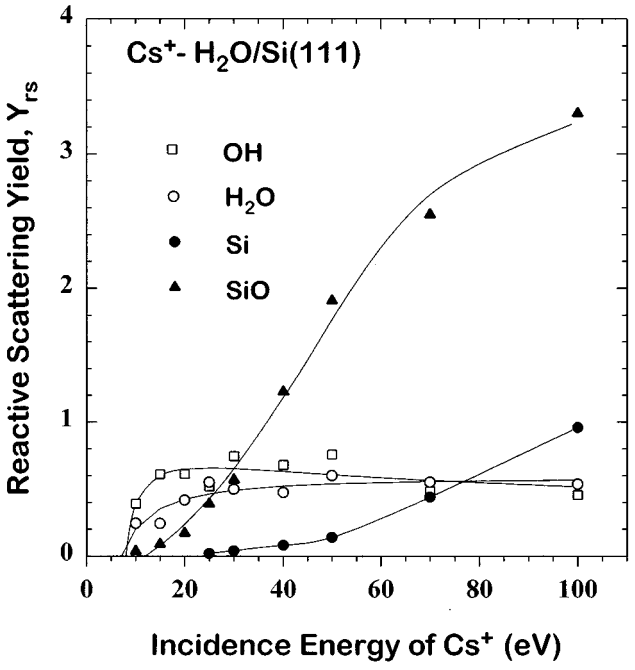

FIG. 3. The reactive scattering yield, $Y_{rs}(X)$, for X=OH (□), H_2O (○), Si (●), and SiO (▲) as a function of Cs^+ beam energy for the range of 10–100 eV. $Y_{rs}(X)$ is normalized to the Cs^+ flux that scatters into a detector solid angle. The curves for $Y_{rs}(OH)$ and $Y_{rs}(H_2O)$ represent the collisional desorption function (see the text).

tensity. Although CsH^+ signal would be buried in the tail of scattered Cs^+ peak, the CsD^+ position is well separable from the Cs^+ tail.

An increase of Cs^+ collision energy to 50 eV strongly increases the yield for $CsSiO^+$ relative to $CsOH^+$ and $CsOH_2^+$ [Fig. 1(c)]. At the same time, the peaks corresponding to $CsSi^+$, $CsSiH^+$, and $CsSiH_2^+$ start to appear at 161, 162, and 163 amu, respectively. The intensity ratio $I(CsOH^+)/I(CsOH_2^+)$ remains unchanged upon this energy increase.

B. Energy-dependency of Cs^+ reactive scattering

The dependency of CsX^+ production yield on Cs^+ collision energy is closely related to the dynamics of reactive scattering. The intensities for Cs^+, $CsOH^+$, $CsOH_2^+$, $CsSi^+$, and $CsSiO^+$ are measured as a function of collision energy for 10–100 eV from the water-saturated surface. $I(CsX^+)$, the quantity presented in Fig. 2, represents the scattered ion intensity normalized to the incident Cs^+ current measured at the sample. $I(Cs^+)$ initially increases with beam energy, then reaches a maximum at about 30 eV. At higher energies $I(Cs^+)$ decreases again. The energy-dependencies for $I(CsOH^+)$ and $I(CsOH_2^+)$ approximately follow the track of the Cs^+ curve. In contrast, $I(CsSi^+)$ and $I(CsSiO^+)$ are small at low collision energies, but continuously increase with increasing energy.

A more useful way of presenting the ion intensity data is to show the reactive scattering yield or reaction probability, $Y_{rs}(X)$, which is defined as the ratio $I(CsX^+)/I(Cs^+)$. $Y_{rs}(X)$ is normalized to the Cs^+ flux that scatters toward a detector angle, and has two advantages over $I(CsX^+)$. First, uncertainty of measuring the incident Cs^+ flux is canceled out in $Y_{rs}(X)$. Due to the very low efficiency for Cs^+ neutralization on Si, it is difficult to deduce the number of incident Cs^+ ions from sample current. Second, the unknown angular distribution for scattered Cs^+ is not problematic, because only the scattering fluxes moving in the same direction (the detector angle) are included in this expression. These two features allow easier analysis for the scattering data in terms of the reactive scattering mechanism. Since the reactive scattering process can conceptually be divided into two steps, collision-induced desorption of X and Cs^+–X association reaction (reactions 1 and 2), we can write

$$Y_{rs}(X)=\frac{I(CsX^+)}{I(Cs^+)}=Y_d(X)Y_{assoc}(X). \quad (1)$$

Here, $Y_d(X)$ is the probability for collisional desorption of X, $I(X)/I(Cs^+)$, and $Y_{assoc}(X)$ is the probability for Cs^+–X association after X desorption, $I(CsX^+)/I(X)$.

The plot of $Y_{rs}(X)$ as a function of beam collision energy is shown in Fig. 3. $Y_{rs}(OH)$ and $Y_{rs}(H_2O)$ increase sharply below 15 eV, then flatten above 20 eV. $Y_{rs}(Si)$ and $Y_{rs}(SiO)$ exhibit quite different behaviors from $Y_{rs}(OH)$ and $Y_{rs}(H_2O)$. $Y_{rs}(Si)$ is virtually zero below 20 eV, and in-

creases slowly and continuously with increasing energy. $Y_{rs}(SiO)$ exhibits an onset at about 10 eV, then a strong increase.

The $Y_{rs}(OH)$ and $Y_{rs}(H_2O)$ data are attempted for a fit with a functional form for collisional desorption cross section. Note that $Y_{rs}(X)$ gives a measure for $Y_d(X)$ [Eq. (1)], under approximation that $Y_{assoc}(X)$ is constant. $Y_d(X)$ can be replaced with desorption cross section $\sigma_d(X)$ for a fixed surface coverage θ, which is the case in the present experiment. We use a collisional desorption model, $\sigma_d(E)=a(E-E_{th})^b/E$,[38] where E is the collision energy, E_{th} is the threshold energy for desorption, and a and b are fitting parameters. This model has been used to determine E_{th} for adsorbate desorption induced by Xe collision.[19] From the fitting we obtain $E_{th}=8.0\pm1.4$ eV for desorption of OH and 7.1 ± 1.8 eV for H_2O. The optimized fitting constants are $a=1.2\pm0.5$ and $b=0.7\pm0.1$ for OH, and $a=0.4\pm0.2$ and $b=1.0\pm0.1$ for H_2O. Whether or not an experimental threshold energy for desorption can be converted into an absolute surface binding energy is probably left to further investigation.[39] At least, this analysis indicates that both H_2O and OH have comparable desorption energies. The curves for $Y_{rs}(Si)$ and $Y_{rs}(SiO)$ cannot be fitted into the $\sigma_d(E)$ form for the entire energy range.

C. Dependency on adsorbate coverage

The variation in $Y_{rs}(X)$ with water exposure is presented in Fig. 4 for OH, H_2O, and SiO. The amount of water exposure was varied from 0 to 1000 L at room temperature. The water vapor pressure was read from an ionization gauge without further calibration. The measurements were performed at 30 eV collision energy, at which the ion intensities are substantial for $CsSiO^+$ as well as for $CsOH^+$ and $CsOH_2^+$. The $Y_{rs}(X)$ curves for these species qualitatively follow the Langmuir adsorption behavior, with an initial stiff increase and a saturation at higher exposures. The curves are fitted by the Langmuir adsorption equation,

$$\theta=1-e^{-cL}, \tag{2}$$

where θ is adsorbate coverage, c fitting constant, and L the amount of water exposure in Langmuir. $Y_{rs}(OH)$ and $Y_{rs}(H_2O)$ fit to the Langmuir equation with $c=0.01\ L^{-1}$. The curve for $Y_{rs}(SiO)$ rises much more steeply and reaches an earlier saturation (<100 L). The $Y_{rs}(SiO)$ fit gives $c=0.2\ L^{-1}$. The early saturation for SiO implies that formation of surface silicon oxides, which are the likely precursors for SiO desorption (Sec. IV C), follows different kinetics from OH and H_2O adsorption.

D. Kinetic energy of scattered ions

Kinetic energies of the scattered ions are measured using a RFA method. A kinetic energy distribution is obtained from raw RFA data through differentiation with respect to energy. Figure 5 shows kinetic energy distributions for Cs^+, Si^+, $CsSi^+$, $CsSiO^+$, and Cs_2^+ emitted during 100 eV Cs^+ collision onto a Si(111) surface with partial H_2O adsorption. $CsOH^+$ and $CsOH_2^+$ have relatively too low signal intensities at the present energy and coverage to accumulate the energy distributions. A 45°/45° specular scattering geometry is employed. The scattered Cs^+ has an energy distribution peaking at about 10 eV. This value indicates that 90% of the Cs^+ beam energy is transferred to the Si surface during 100 eV collision, in agreement with our previous measurement.[40] $CsSi^+$, $CsSiO^+$, and Cs_2^+ are ejected with relatively lower kinetic energies, peaking at 3–5 eV. Monomer Si^+ ions are also ejected with substantial intensity at this relatively high collision energy. The energy distribution for Si^+ exhibits a maximum at about 6 eV, which is slightly higher than the cluster species.

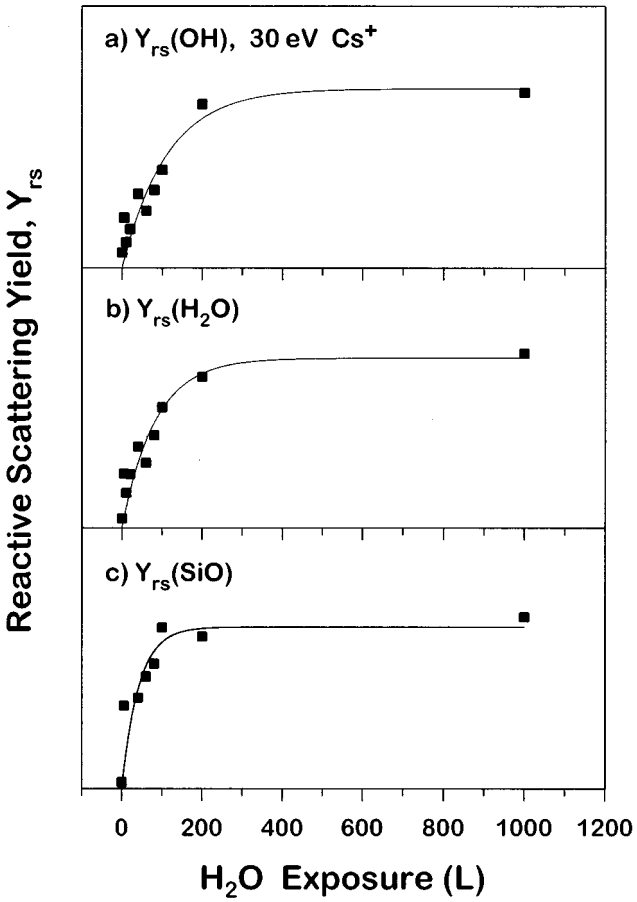

FIG. 4. $Y_{rs}(X)$ for X=OH (a), H_2O (b), and SiO (c) as a function of H_2O exposure in Langmuir. Cs^+ beam energy is 30 eV. The solid lines represent Langmuir adsorption curves.

Although the maximum kinetic energies for the CsX^+ clusters are much lower than that for Cs^+, there are small but sizable overlaps between the energy distributions for Cs^+ and the clusters. The cluster energy distributions are similar to those of sputtered particles, for instance, the sputtered Ni atoms in 100 eV Xe collision on Ni(100) (Ref. 41) and the sputtered Rh atoms in keV Ar^+ bombardment on Rh(111).[42] The kinetic energies for Si^+ appears overall shifted to the high-energy side compared to the clusters or the sputtered atoms. The high-energy shift of ionic Si^+ distribution is probably due to preferential neutralization of the sputtered,

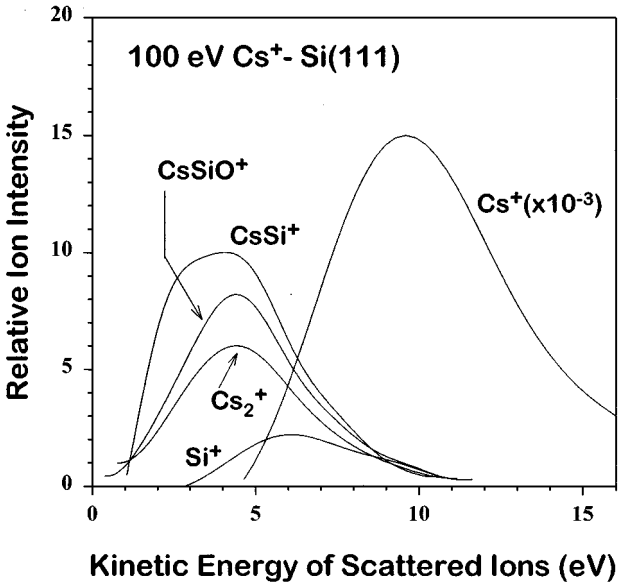

FIG. 5. Kinetic energy distributions for scattered Cs^+, sputtered Si^+, and the cluster species ($CsSi^+$, $CsSiO^+$, and Cs_2^+) produced from a Si surface partially covered with H_2O. The incident Cs^+ energy is 100 eV in a 45°/45° specular scattering geometry. The area under the curves represents relative intensity for the ions.

low energy Si^+ at the surface.[43] Such neutralization effect has been found[40,44] to deplete the low-energy part of the energy distribution for sputtered ions.

Kinetic energy measurement requires extensive signal accumulation be done in order to obtain reasonable statistics for an energy distribution. In such an experiment, a prolonged Cs^+ beam exposure (>several min) deposits a substantial amount of Cs on the surface. The deposited Cs is indicated by the Cs_2^+ emission, formed via reactive scattering from surface Cs. In the presence Cs deposits, an alternative reaction could occur between the sputtered Cs^+ and the desorbed X, also forming the CsX^+ products. A control experiment using 100 eV Ar^+ bombardment on the same surface, covered with both Cs and water, gives extremely small yields for CsX^+ emission. Therefore, we conclude that most of the CsX^+ clusters are produced by reacting with incident Cs^+ beams even in the presence of surface Cs.

IV. DISCUSSION

In the following sections, we will first address two key steps of Cs^+ reactive scattering, collision-induced desorption and ion–molecule association reaction. Then, the experimental observations are analyzed in view of this scattering mechanism. Finally, prospects of doing surface analysis with Cs^+ reactive scattering are discussed.

A. The probability for desorption induced by hyperthermal collision

Desorption induced by low energy ion impact of a surface has been investigated by several workers.[11–13,18,39] Particularly useful to the present study are the reports on desorption yield upon heavy projectile-light surface collision.

TABLE I. Desorption yields upon impact of heavy projectiles on light-atom surfaces at 50–100 eV reported in the literature.

Impact energy	Projectile-surface			
	Kr^+–Ge(s)[a]	Hg^+–Ni(s)[a]	Xe^+–N/W(s)[b]	Xe–Ni(100)[c]
50 eV	0.02	0.01	0.11	0.0(0.0)
100 eV	0.10	0.05	0.24	0.25(0.0)

[a]Reference 12. Ion incidence direction is random.
[b]Reference 13. The desorption yield for adsorbed N atom. Ion incidence direction is random.
[c]Reference 14. Beam incidence angle is 45°. The normal incidence values are in parentheses.

Relevant literature data for the desorption yield, Y_d, are listed in Table I for impact energies of 50 and 100 eV. Y_d values for 50 eV ion impact lie between 0.01–0.02 for surface atom desorption from metal (Ni) and semiconductor (Ge) surfaces. For desorption of chemisorbed N atom from W by Xe^+ collision, it is 0.11. These values are obtained for ion incidence at random directions. The Y_d values are expected to be somewhat different for 45° beam incidence, but probably have the same order. The desorbed species in the present work are Si atoms or chemisorbed species on Si. For such cases, we may assume that Y_d values are similar to or greater than those of Table I, which gives the order Y_d(Si) $\sim$0.01 and Y_d(adsorbate)$\sim$0.1 as lower limits for 50 eV collision.

From the ion intensities of Fig. 1(c), we obtain the probability of reactive scattering, $Y_{rs}(X)$, to be 5×10^{-4} (X=OH and H_2O), 2×10^{-4} (Si), and 2×10^{-3} (SiO) for 50 eV Cs^+–surface collision. Since $Y_{rs}(X)=Y_d(X)Y_{assoc}(X)$ [Eq. (1)], one can deduce from these numbers the probability of Cs^+–X association, $Y_{assoc}(X)$. $Y_{assoc}(X)$ is estimated for the above species to be in the range 5×10^{-3}–2×10^{-2}, if we use Y_d(Si)$\sim$0.01 and Y_d(adsorbate)$\sim$0.1.

B. Ion–molecule association reaction

Since Cs^+ is a chemically inert species, the binary association reaction between the scattered Cs^+ and the desorbed X is to be driven by electrostatic ion–molecule interactions. The binding energy for a Cs^+–OH_2 pair is 0.61 eV,[45] which stands for a typical ion–dipole attraction energy. Cs^+–X association will occur when Cs and X have similar velocities and moving directions such that the energy of their relative motions can be smaller than the ion–molecule binding energy. Figure 5 shows that a major portion of scattered Cs^+ ions has kinetic energy higher than that of CsX^+ clusters. Thus, only a small, low energy portion of the Cs^+ ions, roughly 10% when estimated from the overlapped area between the energy distributions for Cs^+ and CsX^+, appears to meet the energy requirement for cluster formation.

Nonetheless, Cs^+ is the most suitable projectile for reactive scattering among the alkali metal ions. It is because Cs^+ scatters from a surface with substantially lower kinetic energy than other ions due to its heavy mass.[40] We observed in a control experiment with K^+ that the yield for KX^+ production was much smaller.

The association reaction will occur with highest probability while the scattered Cs^+ and the desorbed X are in close locations near the surface. If Cs^+ and X are sufficiently close to each other at the initial stage of attraction, then the nascent Cs^+–X pair will remain stable along its outgoing trajectory. Otherwise, the CsX^+ needs to be energetically stabilized by interacting with the surface and by losing its excess energy. Molecular dynamics (MD) calculations of Xe scattering from a Si surface[40,41] show that 10 eV Xe atoms stay within 3 Å distance from the surface for a period of 2×10^{-13} s. This implies that the Cs^+–X association and the energy quenching is completed most likely within 1 ps. Previously, formation of Cu_n clusters has been studied using a MD method during 600 eV Ar^+ bombardment of a Cu surface.[46] The Cu_n clusters are generated only from the sputtered atoms in this case, but this analogous study has also shown that cluster formation occurs mostly within 4 Å distance from the surface and within 2×10^{-13} s.

The probability for Cs^+–X association is estimated to be 5×10^{-3}–2×10^{-2} in Sec. IV A. An order-of-magnitude calculation may be useful to check the validity of this Y_{assoc} value. The Langevin cross section for reaction between an ion and a nonpolar molecule, $\sigma=\pi_e(2\alpha/E_{\text{rel}})^{1/2}$, has an order of 10 Å^2 for relative motion energy (E_{rel}) of 1 eV and molecular polarizability (α) of 1 Å^3. We assume that about 10% of scattered Cs^+ has kinetic energy small enough to form a stable complex by Cs^+–X interaction, a value estimated from the energy distribution curves of Fig. 5. In this case, in order to give the ion-molecule reaction probability of 5×10^{-3}–2×10^{-2} for scattered Cs^+, molecular gas density of 0.1–0.01 molecule Å^{-3} is required. 10–100 Å^3 is a reasonable volume of space in which a desorbing molecule spreads out during the time scale of reactive scattering, and is consistent with the cluster formation in the near-surface region suggested by the MD calculation.[46]

C. Dynamics of collisional desorption

The energy-dependencies of $Y_{\text{rs}}(\text{OH})$ and $Y_{\text{rs}}(H_2O)$ fit well to the functional form for collisional desorption cross section,[38] $\sigma_d(E)=a(E\text{-}E_{\text{th}})^b/E$. This function is derived from a line-of-centers collision model assuming direct, hard-sphere collisions between a projectile and surface atoms. Thus, its application is limited most likely to desorption of top-layer species. OH and H_2O adsorb on top of a Si surface.[26] The energy-dependencies of $Y_{\text{rs}}(\text{OH})$ and $Y_{\text{rs}}(H_2O)$, a stiff increase at low energy with a plateau at high energy, resemble that of N atom ejection from a W surface during He^+ bombardment reported by Winters and Sigmund.[13] Based on trajectory calculation, they analyzed that the surface N atoms are ejected mostly via direct knock-off collisions with He^+. The agreement of Y_{rs} behavior with the line-of-centers collision model and the N atom ejection from W suggests that OH and H_2O desorb by direct knock-off collisions.

The knock-off ejection of adsorbates by Cs^+ collision might appear unreasonable in view of the sputtering mechanism proposed for keV ion bombardment;[47] heavy ion impact causes the secondary particles to be ejected preferentially as a result of complex collision cascades rather than via direct collisions. However, the situation can change for hyperthermal collision. It has been found[13,41] that as the impact energy is lowered (<100 eV), the directly knocked-off particles have a more dominating portion in the sputtered flux.

It is worthwhile to consider the possibility for the interconversion between H_2O and OH during Cs^+–surface collision. A heavy projectile like Cs^+ distributes its incidence energy to many surface atoms during the collision,[40] and thus the amount of energy transferred to individual atoms should be very small. For this reason, it will be difficult to break HO–H bond [D^0(HO–H)=5.2 eV] by low energy Cs^+ collision, for instance, at <20 eV. A small relative collision energy between Cs^+ and H atoms (0.8% of the Cs beam energy) coming from their extreme mass difference is another drawback for collisional dissociation. More importantly, OH desorption requires dissociation of a HO–H bond, and then desorption of the OH fragment, because H_2O is chemisorbed on Si through O–Si bonding.[26] Such simultaneous fragmentation and ejection requires even higher energy. In Fig. 3, the ratio $Y_{\text{rs}}(\text{OH})/Y_{\text{rs}}(H_2O)$ stays fairly unchanged over a wide energy range. If HO–H bond dissociation occurred to substantial degrees, then it would be reflected by a change in the $Y_{\text{rs}}(\text{OH})/Y_{\text{rs}}(H_2O)$ ratio. All these considerations indicate that both OH and H_2O are present on the surface, which desorb by the collision retaining their original state.

$Y_{\text{rs}}(\text{Si})$ and $Y_{\text{rs}}(\text{SiO})$ exhibit different energy-dependencies from $Y_{\text{rs}}(\text{OH})$ and $Y_{\text{rs}}(H_2O)$ (Fig. 3), suggesting that desorption of Si and SiO involves different mechanism. The curves for $Y_{\text{rs}}(\text{Si})$ and $Y_{\text{rs}}(\text{SiO})$ resemble that for secondary particles ejected via so called substrate sputtering mechanism,[13,41] which is initially low at small impact energy but increases continuously with energy. The substrate sputtering occurs such that the impact energy is initially transferred to substrate atoms, and then eventually to the ejecting species.[13] Subsurface atoms are ejected exclusively via this mechanism.[13,41] For desorption of Si atoms, as they are located underneath the adsorbate layer on the present surface, the substrate sputtering mechanism provides a reasonable explanation.

Desorption of SiO can be related to the presence of silicon oxides on the surface. Recent XPS study[36] has suggested that insertion of O into Si–Si bond occurs upon H_2O exposure on Si(111)-7×7. For saturation exposure at 300 K, the ratio of Si^+/Si^{2+} is 1/0.18. Here, Si^+ is assigned to the surface Si atoms on which only OH is bonded, and Si^{2+} to the OH-decorated adatoms with additional O atom insertion into their Si–Si backbonds.[36] According to this proposed structure, the oxide units (Si–O–Si) are located in the subsurface layer. To be consistent with this structure and the $Y_{\text{rs}}(\text{SiO})$ behavior, we suggest that SiO is generated from the Si–O–Si units via substrate sputtering mechanism. SiO species are known to readily desorb upon heating a water-exposed Si surface,[34] indicating that SiO is a volatile species.

At high collision energy (>30 eV), $Y_{\text{rs}}(\text{SiO})$ becomes larger than $Y_{\text{rs}}(\text{OH})$ or $Y_{\text{rs}}(H_2O)$. Since the surface popula-

tion of the oxides should be considerably smaller than OH and H_2O according to the XPS study,[36] the observation of large $Y_{rs}(SiO)$ is difficult to reconcile. One possible explanation is that the efficiency for SiO ejection drastically increases at high collision energy. Note that desorption via substrate sputtering much prevails at high energy over direct knock-off ejection of adsorbate.[13,41] Another possibility is collisional conversion of surface OH or H_2O into SiO. SiO formation is thermally a facile reaction on this surface.[34] Thus, if collision cascades are generated in the surface region by high energy impact, then it is plausible to induce SiO desorption.

D. Identification of surface adsorbate

In the previous sections, formation of $CsOH^+$, $CsOH_2^+$, $CsSi^+$, and $CsSiO^+$ has been explained in the framework of collisional desorption of surface adsorbates or atoms followed by association reaction with Cs^+. $CsOH^+$ and $CsOH_2^+$ are formed by direct desorption of chemisorbed OH and H_2O, respectively. $CsOH^+$ and $CsOH_2^+$ show comparable ion intensities. Provided that Y_d and Y_{assoc} are approximately equal for OH and H_2O, the ratio $I(CsOH^+)/I(CsOH_2^+)$ stands for the relative surface population of the two species. $CsSi^+$ production represents sputtering of Si atoms. $CsSiO^+$ produced at low impact energy ($<$20 eV) is related to SiO desorption from the Si–O–Si units present on a water-saturated Si surface. However, the strong increase of $CsSiO^+$ emission with collision energy suggests that other reaction channels possibly intervene during high energy collision.

Atomic hydrogens are believed[29] to exist on the water-exposed Si(111) surface. $CsSiH_n^+(n=1,2)$ peaks of Fig. 1(c) indicate the presence of SiH_n species on the surface. Contrarily, CsD^+ peak is not observed in Fig. 1(b). The absence of CsD^+ peak indicates the difficulty of dissociating the Si–D bond by Cs^+ collision, and likewise the Si–H bond. Because of an extremely small efficiency for energy-transfer from Cs^+ to H, the collision may cause SiH_n desorption rather than dissociation of the Si–H bond. It is also probable that the small molecular polarizability of H atom reduces the Cs^+–H association yield.

It is interesting to compare the Cs^+ reactive scattering with other desorption or sputtering techniques. Temperature programmed desorption (TPD) from the same surface[34] gives rise to H_2O, H_2, and SiO at desorption temperatures of 160, 800, and 950 K, respectively. The existing adsorbates such as OH and H are not thermally desorbed. Apparently, a slow heating rate ($<10\ K\ s^{-1}$) in TPD has caused thermal reactions to occur, desorbing only thermally available products like H_2 and SiO. Laser induced thermal desorption (LITD) (Refs. 33,34) produces H_2 (100%), SiO (80%), SiOH (44%), H_2O (22%), Si (16%), and $Si(OH)_2$ (14%), the numbers in parentheses representing the relative branching ratios. The desorbed products like H_2O, SiOH, and $Si(OH)_n(n=1,2)$ reflect the presence of H_2O and OH on the surface. Due to the rapid heating rate ($>10^{10}\ K\ s^{-1}$), thermal reactions are noticeably suppressed in LITD. However, thermal decomposition still plays an important role, as indicated by desorption of H_2 and SiO.

Secondary ion mass spectrometry (SIMS) from a Si surface reacted with O_2 shows a number of ions including Si^+, Si_2^+, SiO^+, Si_2O^+, $Si_2O_2^+$, Si_3O^+, and etc.[48] Despite numerous superior features of SIMS as a surface analysis technique, identification of molecular adsorbate structure from such a complex spectrum is presently an almost impossible task. One will need to fully account for the probability of secondary particle ionization and the mechanisms of molecular ion ejection and fragmentation occurring during keV ion bombardment.

When compared to the above-mentioned TPD, LITD, and SIMS results, hyperthermal Cs^+ reactive scattering promises has several unique features for adsorbate detection. First, by detecting Cs^+-bound cluster ions, the problem of secondary particle ionization in conventional SIMS can be overcome. The probability of Cs^+–X association (5×10^{-3}–2×10^{-2}) is higher than the efficiencies of molecule ionization normally achievable by keV ion sputtering or by electron impact ionization. The formation of CsX^+ clusters has previously been reported (Cs^+-SIMS),[49–51] and has been utilized for surface compositional analysis. However, the destructive nature of keV sputtering in Cs^+-SIMS hampers molecular adsorbate identification. Second, the reactive scattering occurs in subpicosecond time scale, which is faster than the desorption time in LITD ($\geqslant$ns) by at least three orders. This means that the scattered Cs^+ ions pick up only promptly desorbed molecules. In certain cases, Cs^+ collision may initiate surface chemical reactions that occur in slower time scales. The delayed reaction products, however, will not be able to form CsX^+, and thus not be detected. This scenario explains why thermally unstable species like OH can be monitored by Cs^+ reactive scattering, while it is not the case in LITD and TPD. Third, hyperthermal collision induces molecular fragmentation to a lesser degree than keV sputtering. Hence, molecular identity of an adsorbate is better preserved during the collisional desorption. For the systems where CO, H_2O, and C_6H_6 are chemisorbed on a Ni(100) surface, all these adsorbates are detected in their molecular forms by Cs^+ reactive scattering.[52] We expect that there may be exceptions to exclusive molecular desorption. The strong emission of $CsSiO^+$ observed at high collision energy possibly indicates adsorbate fragmentation. Competition between molecular desorption and fragmentation will be controllable with Cs^+ beam energy depending on chemical property of a system.

V. SUMMARY AND CONCLUSIONS

(1) Hyperthermal collision of Cs^+ ions onto a Si(111) surface reacted with water gives rise to emission of $CsOH^+$, $CsOH_2^+$, $CsSi^+$, $CsSiH_n^+(n=1,2)$, and $CsSiO^+$ ions. These cluster species are formed as a result of collisional desorption of surface species, followed by ion–molecule association between the low-energy scattered Cs^+ and the desorbed molecule.

(2) $CsOH^+$ and $CsOH_2^+$ are proposed to be formed from desorption of OH and H_2O adsorbates, respectively, which occurs via direct knock-off collision with Cs^+. It follows that the OH and H_2O species coexist on the surface with comparable surface concentrations. $CsSi^+$ and $CsSiO^+$ emission suggests desorption of Si and SiO, respectively, via substrate sputtering mechanism.
(3) The probability of reactive scattering is 5×10^{-4}–2×10^{-3} for 50 eV Cs^+ collision on the present surface. The corresponding probability of Cs^+–X association reaction is in the order 5×10^{-3}–2×10^{-2} or slightly lower.
(4) Unique capabilities of Cs^+ reactive scattering as a surface analysis method have been demonstrated. They are (i) detection of desorbed neutral species, (ii) fast probing-time compared to thermal reaction and LITD, and (iii) possibility for molecular adsorbate detection.

ACKNOWLEDGMENTS

The authors thank K. D. Kim and K. Y. Kim for their assistance. This project was financially supported in parts by KOSEF (CMS), ETRI, and School of Environmental Engineering.

[1] F. O. Goodman and H. Y. Wachman, in *Dynamics of Gas–Surface Scattering* (Academic, New York, 1976).
[2] S. R. Kasi, H. Kang, C. S. Sass, and J. W. Rabalais, Surf. Sci. Rep. **10**, 1 (1989).
[3] M. R. Morris, Jr., D. E. Riederer, B. E. Winger, R. G. Cooks, T. Ast, and C. E. D. Chidsey, Int. J. Mass Spectrom. Ion Processes **122**, 181 (1992).
[4] R. G. Cooks, T. Ast, T. Pradeep, and V. Wysocki, Acc. Chem. Res. **27**, 316 (1994).
[5] H. Akazawa and Y. Murata, J. Chem. Phys. **88**, 3317 (1988).
[6] S. Schubert, U. Imke, W. Heiland, K. J. Snowdon, P. H. F. Reijnen, and A. W. Kleyn, Surf. Sci. **205**, L793 (1988).
[7] K. H. Park, B. C. Kim, and H. Kang, J. Chem. Phys. **97**, 2742 (1992).
[8] U. van Slooten, O. M. N. D. Teodore, A. W. Kleyn, J. Los, D. Taillet-Billy, and J. P. Gauyacq, J. Chem. Phys. **179**, 227 (1994).
[9] J. S. Martin, J. N. Greeley, J. R. Morris, B. T. Feranchak, and D. C. Jacobs, J. Chem. Phys. **100**, 6791 (1994).
[10] J. A. Burroughs, S. B. Wainhaus, and L. Hanley, J. Chem. Phys. **103**, 6706 (1995).
[11] G. K. Wehner, Phys. Rev. **108**, 35 (1957); *ibid*. **112**, 1120 (1958).
[12] N. Laegreid and G. K. Wehner, J. Appl. Phys. **32**, 365 (1961); R. V. Stuart and G. K. Wehner, *ibid*. **33**, 2345 (1962).
[13] H. F. Winters and P. Sigmund, J. Appl. Phys. **45**, 4760 (1974).
[14] J. W. Rabalais, T. R. Schuler, and O. Grizzi, Nucl. Instrum. Methods Phys. Res. B **28**, 185 (1987).
[15] J. Murakami and I. Kusunoki, Nucl. Instrum. Methods Phys. Res. B **33**, 560 (1988).
[16] U. Diebold and P. Varga, Surf. Sci. **241**, L6 (1991).
[17] J. D. Beckerle, A. D. Johnson, and S. T. Ceyer, J. Chem. Phys. **93**, 4047 (1990).
[18] C. Kim, J. R. Han, and H. Kang, Surf. Sci. **320**, L76 (1994).
[19] D. Velic and R. J. Levis, J. Chem. Phys. **104**, 9629 (1996).
[20] J. L. Robertson, S. C. Moss, Y. Lifshitz, S. R. Kasi, J. W. Rabalais, G. D. Lempert, and E. Rapoport, Science **243**, 1047 (1989).
[21] H. J. Steffen, D. Marton, and J. W. Rabalais, Phys. Rev. Lett. **68**, 1726 (1992).
[22] B. C. Kim, H. Kang, C. Y. Kim, and J. W. Chung, Surf. Sci. **301**, 295 (1994).
[23] J. R. Hahn, H. Kang, S. Song, and I. C. Jeon, Phys. Rev. B **53**, R1725 (1996).
[24] M. C. Yang, H. W. Lee, and H. Kang, J. Chem. Phys. **103**, 5149 (1995).
[25] M. C. Yang, C. H. Hwang, J. K. Ku, and H. Kang, Surf. Sci. **366**, L719 (1996).
[26] P. A. Thiel and T. E. Madey, Surf. Sci. Rep. **7**, 211 (1987).
[27] K. Fujiwara, Surf. Sci. **108**, 124 (1981).
[28] D. Schmeisser, F. J. Himpsel, and G. Hollinger, Phys. Rev. B **27**, 7813 (1983).
[29] S. Ciraci and H. Wagner, Phys. Rev. B **27**, 5180 (1983).
[30] H. Ibach, H. Wagner, and D. Bruchman, Solid State Commun. **42**, 457 (1982).
[31] M. Nishijima, K. Edamoto, Y. Kubota, S. Tanaka, and M. Onchi, J. Chem. Phys. **84**, 6458 (1986).
[32] D. Schmeisser and J. E. Demuth, Phys. Rev. B **33**, 4233 (1986).
[33] C. H. Mak, B. G. Koehler, and S. M. George, Surf. Sci. **208**, L42 (1989).
[34] B. G. Koehler, C. H. Mak, and S. M. George, Surf. Sci. **221**, 565 (1989).
[35] M. Chander, Y. Z. Li, J. C. Patrin, and J. H. Weaver, Phys. Rev. B **48**, 2493 (1993).
[36] C. Ponccy, F. Rochet, G. Dufour, H. Roulet, F. Sirotti, and G. Panaccione, Surf. Sci. **338**, 143 (1995).
[37] W. Y. Choi, T. H. Kang, and H. Kang, Bull. Kor. Chem. Soc. **11**, 290 (1990).
[38] A. G. Urena, J. Phys. Chem. **96**, 8212 (1992).
[39] W. Eckstein, C. Garcia-Rosales, and J. Roth, Nucl. Instrum. Methods Phys. Res. B **83**, 955 (1993).
[40] M. C. Yang, C. Kim, H. W. Lee, and H. Kang, Surf. Sci. **357**, 595 (1996).
[41] C. Kim, H. Kang, and S. C. Park, Nucl. Instrum. Methods Phys. Res. B **95**, 171 (1995).
[42] B. J. Garrison, C. T. Reimann, N. Winograd, and D. E. Harrison, Jr., Phys. Rev. B **36**, 3516 (1987).
[43] R. F. Garrett, R. J. MacDonald, and D. J. O'Connor, Surf. Sci. **138**, 432 (1984).
[44] H. W. Lee and H. Kang, Bull. Kor. Chem. Soc. **16**, 101 (1995).
[45] P. Kebarle, Annu. Rev. Phys. Chem. **28**, 445 (1977).
[46] B. J. Garrison, N. Winograd, and D. E. Harrison, Jr., J. Chem. Phys. **69**, 1440 (1978).
[47] P. Sigmund, Phys. Rev. **184**, 383 (1969).
[48] A. Benninghoven, W. Sichtermann, and S. Storp, Thin Solid Films **28**, 59 (1975).
[49] H. A. Storms, K. F. Brown, and J. D. Stein, Anal. Chem. **49**, 2023 (1977).
[50] Y. Gao, J. Appl. Phys. **64**, 3760 (1988).
[51] K. Wittmaack, Nucl. Instrum. Methods Phys. Res. B **85**, 374 (1994).
[52] H. Kang, M. C. Yang, K. D. Kim, and K. Y. Kim, Int. J. Mass Spectrom. Ion Processes (submitted).